JOURNAL OF CATALYSIS 104, 147–155 (1987)

A Novel Method for Analyzing Transient Response Data Obtained in Isotopic Tracer Studies of CO Hydrogenation

M. DE PONTES, G. H. YOKOMIZO, AND A. T. BELL

Materials and Molecular Research Division, Lawrence Berkeley Laboratory, and Department of Chemical Engineering, University of California, Berkeley, California 94720

Received July 22, 1986; revised October 14, 1986

A method is described for analyzing transient response data obtained in isotopic tracer studies of CO hydrogenation. Methane is assumed to be produced by the independent hydrogenation of various pools of carbon present on the catalyst surface, but no assumptions are made about the number of such pools nor the homogeneity of their reactivity. Application of the method to data for Ru and Ni catalysts reveals bimodal spectra of first-order rate coefficients. The peaks in these spectra are assigned to specific forms of adsorbed carbon. It is also shown that the ability to resolve different carbon forms and the heterogeneity in the reactivity of these forms is closely linked to the noise in the experimentally observed transients.

INTRODUCTION

The formation of methane from synthesis gas has been shown to proceed via the dissociation of adsorbed CO and subsequent hydrogenation of the nascent carbon (see, for example, Refs. (*1–3*)). Isotopic tracer experiments (*4–14*) and NMR studies (*15, 16*) have demonstrated further that under working conditions Group VIII metal catalysts may have several types of carbon present, which differ in their structure and reactivity. The principal forms are atomic carbon (C_α), short alkyl chains (C_β), and graphitic carbon (C_γ). For Ru it has been established that the surface concentration of C_α comes to a steady state with the same time constant as the rate of CO hydrogenation, and that C_α is the primary precursor to methane and other hydrocarbon products. The surface concentration of C_β builds up more slowly than that of C_α and does not correlate with the rate of product formation. Thus, C_β can be regarded as a reservoir of carbon that is less active than C_α. The formation of C_γ is not observed for low reaction temperatures (i.e., $T \lesssim 498$ K), but is formed at higher temperatures (*11*) or if C_α and C_β are heated in the absence of hydrogen (*17*).

While the relationships of C_α to adsorbed CO and the formation of methane are reasonably well established, the pathways via which C_β is formed and reacts are not yet fully defined. Bell and co-workers (*11, 15*) have proposed that for Ru, C_α and C_β are related as shown in Scheme A:

$$\begin{array}{l} CO_g \rightleftarrows CO_a \rightarrow C_\alpha + O_s \\ \qquad\qquad\quad {\scriptstyle +H_a}\uparrow\downarrow{\scriptstyle -H_a} \\ \qquad\qquad\quad [CH_x] \rightleftarrows C_\beta \\ \qquad\qquad\quad {\scriptstyle H_a}\downarrow \\ \qquad\qquad\quad CH_4 \end{array}$$

A similar scheme has also been proposed by Happel and co-workers (*9*) for Ni. In a recent study of CO hydrogenation over Raney Ni, Soong *et al.* (*14*) have proposed that in addition to Scheme A, one should consider Schemes B and C shown below:

$$\begin{array}{l} CO_a \rightarrow C_\alpha \xrightarrow{H_a} CH_4 \\ \qquad\quad \uparrow\downarrow \\ \qquad\quad C_\beta \xrightarrow{H_a} CH_4 \end{array} \qquad\qquad \begin{array}{l} \qquad\quad C_\alpha \xrightarrow{H_a} CH_4 \\ CO \nearrow\ \downarrow\downarrow \\ \qquad\quad C_\beta \xrightarrow{H_a} CH_4 \end{array}$$

An important point brought out by these authors is that the equations describing the transient response of these networks to a sudden change in the isotopic label of carbon are identical in form. Consequently, it is not possible to distinguish between the

0021-9517/87 $3.00

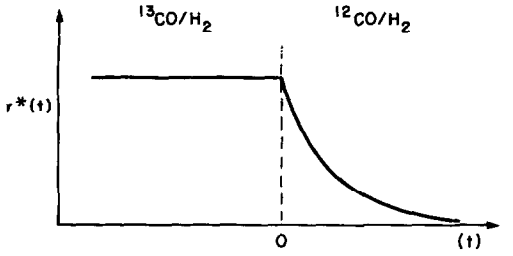

FIG. 1. An illustration of the response in the rate of $^{13}CH_4$ formation during an isotopic-tracer experiment. The switch in feed composition from $^{13}CO/H_2$ to $^{12}CO/H_2$ is made at $t = 0$.

three schemes on the basis of transient experiments alone. Because of this, Soong *et al.* (*14*) analyzed their data assuming that C_α and C_β react to methane along parallel, independent pathways.

The kinetics of carbon hydrogenation to methane have been assumed by previous authors (*7, 9–11, 14*) to be first order in carbon coverage and characterized by a single rate coefficient for each form of adsorbed carbon. The latter assumption implies that all atoms in a given class have the same reactivity. We believe this assumption to be overly restrictive. Recent NMR evidence (*15*) suggests that carbidic carbon atoms are present in a variety of environments. As a consequence, one might reasonably expect carbidic carbon, as well as other carbon forms, to exhibit a spectrum of reactivities with adsorbed hydrogen. In the present paper, we propose that the hydrogenation of adsorbed carbon be described by a spectrum of first-order rate coefficients and show how to determine this spectrum from isotopic-tracer experiments. Our method of data analysis requires no assumptions regarding the number of carbon classes, the distribution of carbon between classes, or the homogeneity of reactivity for carbon atoms in a given class.

METHOD OF DATA ANALYSIS

Before describing the method of data analysis, it is useful to review the procedure used to acquire transient-response data and the assumptions underlying their interpretation. Fig. 1 illustrates the sequence of steps involved in a typical isotopic-tracer experiment.

The catalyst is first exposed to a mixture of ^{13}CO and H_2 for a fixed period of time. At time $t = 0$, the feed is switched to a mixture of ^{12}CO and H_2, without altering the partial pressures or flow rates of either reactant. Assuming that the reactor space time is much shorter than the reaction system response time, the switch in feeds at $t = 0$ imposes a step function change in the isotopic composition of the gas-phase CO present over the catalyst. Since the CO and H_2 remain constant throughout the experiment, the coverage of all adsorbed species remains constant. For carbon, this situation can be represented by

$$\theta_{^{13}C} + \theta_{^{12}C} = \theta_C = \text{const.} \qquad (1)$$

where $\theta_{^{13}C}$, $\theta_{^{12}C}$, and θ_C are the surface coverages of ^{13}C, ^{12}C, and total carbon, respectively.

The decay in the rate of $^{13}CH_4$ production for $t > 0$ is due to the depletion of ^{13}C-containing species (e.g., ^{13}CO, $^{13}C_\alpha$, $^{13}C_\beta$) from the catalyst surface. Since the exchange of adsorbed ^{13}CO for ^{12}CO has been found experimentally (*7, 11–13*) to be much more rapid than the rate of methane formation, the majority of the $^{13}CH_4$ observed during the transient response derives from the hydrogenation of $^{13}C_\alpha$ and $^{13}C_\beta$, the hydrogenation of adsorbed ^{13}CO contributing to only the first few seconds of the transient.

To simulate the transient response shown in Fig. 1, it is necessary to make some assumptions about the distribution of carbon species on the catalyst surface, the homogeneity in reactivity of each carbon species, and the connectivity between species. If, for example, there is only one form of carbon with a uniquely defined reactivity, then the rate of $^{13}CH_4$ formation as a function of time, $r^*(t)$, is given by

$$r^*(t) = \theta_0^* k e^{-kt}, \tag{2}$$

where θ_0^* is the initial coverage of ^{13}C-labeled carbon and k is the first-order rate coefficient. For the case of P pools of carbon, each of which can react independently, the expression for $r^*(t)$ becomes

$$r^*(t) = \sum_{i=1}^{P} \theta_0^* x_i k_i e^{-k_i t}, \tag{3}$$

where x_i is the fraction of ^{13}C-labeled carbon in pool i at time zero and k_i is the rate coefficient for carbon in pool i. If the number of carbon pools becomes very large and/or the reactivity of carbon in a given pool is not uniquely defined, x_i in Eq. (3) can be replaced by $dx = f(k)dk$, where $f(k)dk$ gives the probability that carbon atoms have rate coefficient between k and $k + dk$. The total rate of $^{13}CH_4$ formation at any time during the transient can then be represented by

$$r^*(t) = \theta_0^* \int_0^\infty k f(k) e^{-kt} dk. \tag{4}$$

Equation (4) is identical to that written by Scott (*18*) to describe the time-dependent reaction of a preadsorbed reactant for situations where there is a distribution of catalytically active sites.

For the present study we assume that $r^*(t)$ is given by Eq. (4). The objective is to then find $f(k)$ such that Eq. (4) describes the experimentally observed values of $r^*(t)$. Two approaches are possible. The first is to assume an analytical expression for $f(k)$ and to then adjust the parameters appearing in this function so as to obtain a fit between theory and experiment (*18*). The difficulty here is that there is no physical basis for choosing the form of $f(k)$. The second approach starts by recognizing that $r^*(t)$ represents the Laplace transform of $\theta_0^* k f(k)$. One could, therefore, determine $f(k)$ by taking the inverse Laplace transform of the experimental values of $r^*(t)$ and then dividing it by $k\theta_0^*$. The difficulty in this case is that noise in the time-dependent signal can cause large errors in the computed value of the inverse Laplace transform (*19, 20*).

Since the second of the two methods described above requires no a priori assumptions about the form of $f(k)$, it is more appealing. The question then is how can $f(k)$ be found with the greatest accuracy for a given level of noise in $r^*(t)$. This problem can be addressed in a rigorous manner using the approach described recently by McWhiter (*21*) and Ostrowsky *et al.* (*22*). A summary of their method is given in the Appendix.

Application of the development given by Ostrowsky *et al.* (*22*) to Eq. (4) leads to the following representation of $r^*(t)$

$$r^*(t) = \sum_{n=1}^{N} \left(\frac{\pi}{\omega_{\max}}\right) \theta_0^* k_n^2 f(k_n) \exp(-k_n t) W_{\omega_{\max}}(k_n, t), \tag{5}$$

where

$$k_{n+1} = k_1 \exp(n\pi/\omega_{\max}) \tag{6}$$

and

$$W_{\omega_{\max}}(k_n, t) = \int_{\log k_1}^{\log k_N} \exp[-t(k - k_n)] \exp[\tfrac{1}{2} \log(k/k_n)] \frac{\sin[\omega_{\max} \log(k/k_n)] d(\log k)}{\pi \log(k/k_n)}. \tag{7}$$

Thus, $r^*(t)$ is represented with a finite number of values of k_n, spaced logarithmically between k_1 and k_N. The parameter $\omega_{\max}$ which defines the spacing between adjacent values of k_n can be estimated from the noise in $r^*(t)$, ε, using the relation (see Appendix)

$$\varepsilon \simeq \sqrt{\frac{\pi}{\cosh(\pi\omega_{\max})}}. \tag{8}$$

Ostrowsky *et al.* (*22*) have shown that $W_{\omega_{\max}}(k_n, t)$ goes to 1, in the limit $\omega_{\max} \to \infty$, and in practice $W_{\omega_{\max}}(k_n, t) \simeq 1$ for $\omega_{\max} \geq 3$ (i.e., $\varepsilon \leq 0.02$). With this approximation, Eq. (5) can be simplified to read

$$r^*(t) = \sum_{n=1}^{N} a_n \exp(-k_n t), \tag{9}$$

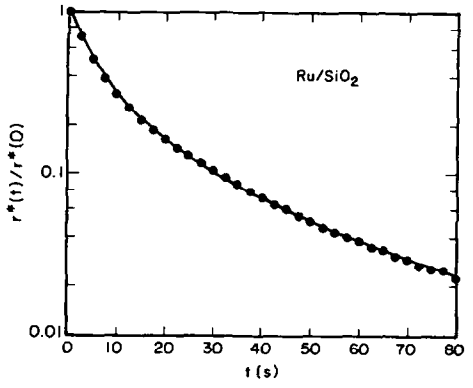

FIG. 2. The transient response observed for Ru/SiO_2 upon switching to $^{12}CO/D_2$ following a 30-s exposure to $^{13}CO/D_2$: $T = 363$ K; $P = 1$ atm; $D_2/CO = 3$. The solid line represents a fit of Eq. (9) to the data.

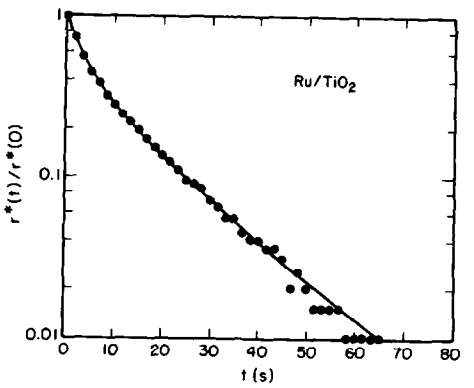

FIG. 3. The Transient response observed for Ru/TiO_2 upon switching to $^{12}CO/D_2$ following a 30-s exposure to $^{13}CO/D_2$: $T = 363$ K; $P = 1$ atm; $D_2/CO = 3$. The solid line represents a fit of Eq. (9) to the data.

where

$$a_n = \frac{\pi}{\omega_{\max}} \theta_0^* k_n^2 f(k_n). \qquad (10)$$

The values of a_n in Eq. (9) can be determined by carrying out a least-squares fit of Eq. (9) to experimental values of $r^*(t)$ measured at M discrete times t_i ($i = 1$ to M). The objective function to be minimized is then

$$\sum_{i=1}^{M} \left[r^*(t_i) - \sum_{n=1}^{N} a_n \exp(-k_n t_i) \right]^2. \qquad (11)$$

Once the values of a_n are known, the values of $\theta_0^* f(k_n)$ can be calculated from Eq. (10).

The utility of the theoretical analysis given above can now be demonstrated. As a first illustration, we shall consider data obtained in this laboratory using SiO_2- and TiO_2-supported Ru catalysts. Isotopic tracer experiments were carried out at 463 K and 1 atm with a D_2 : CO ratio of 3 to 1. The transient response in $^{13}CD_4$ formation following the switch from a mixture of $D_2/^{13}CO$ to $D_2/^{12}CO$ is shown in Figs. 2 and 3. It is evident from the curvature in both semilogarithmic plots that the decay cannot be described by a single time constant, or rate coefficient.

Figures 4 and 5 present plots of $f(k)$ determined from the data given in Figs. 2 and 3. As indicated in the legends for Figs. 4 and 5, the different symbols correspond to different values of k_1; the value of $\omega_{\max}$ in both cases is 3.5. Each plot exhibits a bimodal distribution of rate coefficients. The intensity of the second peak has been set arbitrarily to unity. Mean values of the rate coefficient $\bar{k}$ determined for each peak and the relative peak areas are given in Table I. The right peak can be assigned to the hydrogenation of C_α, whereas the left peak can be assigned to the hydrogenation of C_β. These assignments are based on the obser-

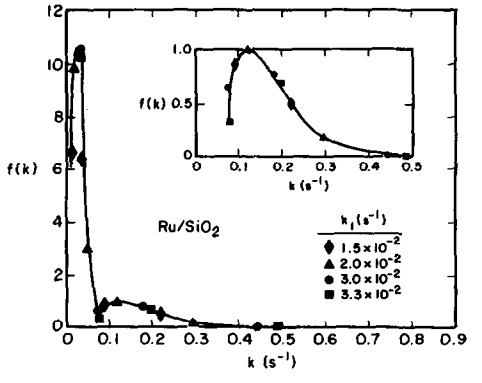

FIG. 4. A plot of $f(k)$ for Ru/SiO_2, based on the data in Fig. 2.

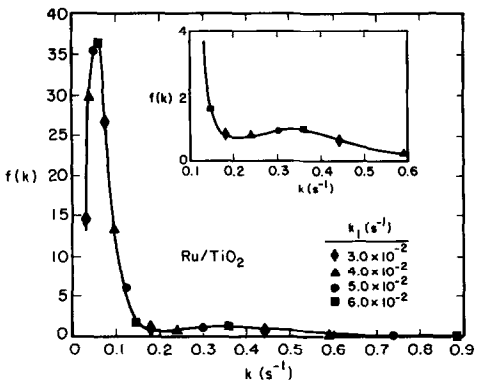

FIG. 5. A plot of $f(k)$ for Ru/TiO_2, based on the data in Fig. 3.

vations of Winslow and Bell (*11*) for Ru/SiO_2, which demonstrated that C_α undergoes hydrogenation more rapidly than C_β.

The results in Table I show that the $\bar{k}$'s for C_α and C_β are about a factor of two greater for Ru/TiO_2 than Ru/SiO_2. The interpretation of this difference must be done with care since the rate coefficient k used in the present analysis is, in fact, the product of the intrinsic rate coefficient and the coverage of the catalyst surface by hydrogen. The latter factor arises from the fact that while the rate of methane formation is first order in carbon, it is also dependent to some power on the hydrogen coverage. Since the hydrogen coverage does not change in the experiments described here, the dependence of the methanation rate on hydrogen coverage is incorporated into k. Consequently, the larger values of $\bar{k}$ for Ru/TiO_2 relative to Ru/SiO_2 may be due either to a higher hydrogen coverage or to higher intrinsic rate coefficients. Without an independent determination of the dependence of $\bar{k}$ on hydrogen coverage, we cannot say which of these effects is dominant.

It is also seen in Table I that for both Ru/SiO_2 and Ru/TiO_2, the relative area for the C_β peak in $f(k)$ is greater than that for the C_α peak. This suggests that even after 30 s of exposure to synthesis gas, the coverage of C_β on both catalysts is greater than that of C_α. Independent measurements of the coverages by C_α and C_β for Ru/SiO_2 (*11*, *15*) are in good agreement with this conclusion. The fact that the ratio of C_β and C_α peak areas is greater for Ru/TiO_2 than Ru/SiO_2 (see Table I) suggests further that the accumulation of alkyl chains (i.e., C_β) occurs more rapidly when Ru is supported on TiO_2. Here too consistency can be found with independent observations. Under identical reaction conditions the probability of chain growth is greater for Ru/TiO_2 than Ru/SiO_2 (*23*).

The solid curves in Figs. 2 and 3 are based on Eq. (9). In determining these curves, the values of $f(k)$ indicated by the ● symbols in Figs. 4 and 5 were used. It is evident that for both exposure times, Eq. (9) provides a very good description of the experimental data. Equivalent fits of the data were obtained if values of $f(k)$ corre-

TABLE I

Average Rate Coefficients and Mole Fractions for C_α and C_β

Catalyst	$\bar{k}_{C_\beta}(s^{-1})$	$\bar{x}_{C_\beta}$	$\bar{k}_{C_\alpha}(s^{-1})$	$\bar{x}_{C_\alpha}$	Ref.
Ru/SiO_2	3.3×10^{-2}	0.67	1.8×10^{-1}	0.33	This work
Ru/TiO_2	7.1×10^{-2}	0.89	4.1×10^{-1}	0.11	This work
Raney Ni	6.3×10^{-4}	0.30	3.8×10^{-3}	0.70	Soong *et al.* (*14*)
Raney Ni	1.2×10^{-3}[a]	—	8.3×10^{-3}[a]	—	Soong *et al.* (*14*)
Raney Ni	2.3×10^{-3}[b]	—	8.9×10^{-3}[b]	—	Soong *et al.* (*14*)

[a] Determined from the time constants reported by Soong *et al.* (*14*).
[b] Determined by fitting Eq. (12) to the data of Soong *et al.* (*14*).

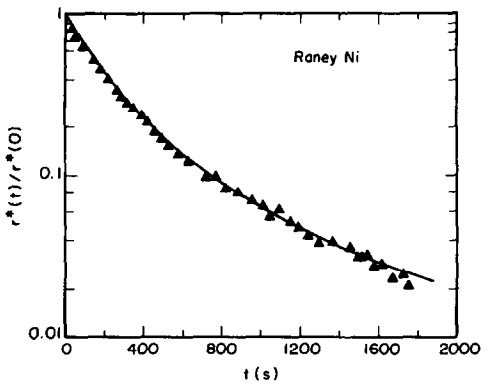

FIG. 6. The transient response observed by Soong *et al.* (*14*) for Raney Ni upon switching to $^{12}CO/H_2$ following a 480-s exposure to $^{13}CO/H_2$ (*14*): T = 383 K; P = 1 atm; H_2/CO = 2. The solid represents a fit of Eq. (9) to the data.

sponding to one of the other symbols appearing in Figs. 4 and 5 were used. What this indicates is that the quality of the fit of the experimental data is independent of the value of k_1 chosen in Eq. (6).

The method of data analysis proposed here has also been used on data obtained for Raney Ni by Soong *et al.* (*14*). Fig. 6 shows the decay in methanation rate. The corresponding plots of $f(k)$ is given in Fig. 7 and the characteristic features of the plot are listed in Table I. Figure 7 again show a bimodal distribution of k. The ratio of mean k values for the C_α and C_β peaks are comparable to those observed for Ru/TiO_2, but the ratios of peak areas is smaller. The much smaller accumulation of C_β relative to C_α observed for Ni is consistent with the fact that chain growth does not occur as readily on Ni as on Ru.

The average values of the rate coefficients for C_α and C_β obtained here for the data of Soong *et al.* (*14*) can be compared with those reported by these authors. Soong *et al.* (*14*) obtained a value of k for C_α from transient responses taken after a short (120-s) preexposure to the $^{13}CO/H_2$ mixture. It was assumed that since the preexposure time was short, little C_β would have built up and hence influenced the determination of the time constant for C_α. The value of k for C_β was then obtained by fitting a model for the parallel decay of two carbon reservoirs to transient responses taken after a long (2000-s) preexposure to the $^{13}CO/H_2$ mixture. The values of k obtained in this fashion by Soong *et al.* (*14*) are listed in Table I.

It is evident from Table I that the value of k for C_α obtained by Soong *et al.* (*14*) is significantly larger than that reported here. The principal reason for this difference is the difference in the methods of data analysis. In particular if the short preexposure experiments used by Soong *et al.* (*14*) to determine the value of C_α contained some C_β, this would lead to an underestimation of k and C_α and, in turn, to an overestimation of k for C_β. The present method of data analysis is not influenced by such considerations, since no a priori assumptions are required about the distribution of C_α and C_β. It is, therefore, the opinion of the present authors that the resulting values of k more accurately reflect the intrinsic reactivity of the different forms of carbon present on the catalyst surface. It should be noted further that while the data of Soong *et al.* (*14*), shown in Fig. 6, are very well represented by Eq. (9) and the distribution of rate coefficients given in Fig. 7, the representation of the data by a weighted sum of two exponentials is not as good. Figure 8

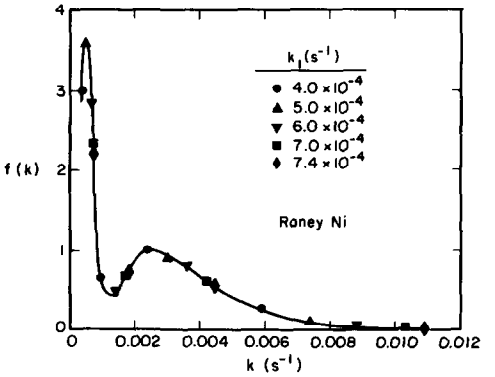

FIG. 7. A plot of $f(k)$ for Raney Ni, based on the data in Fig. 6.

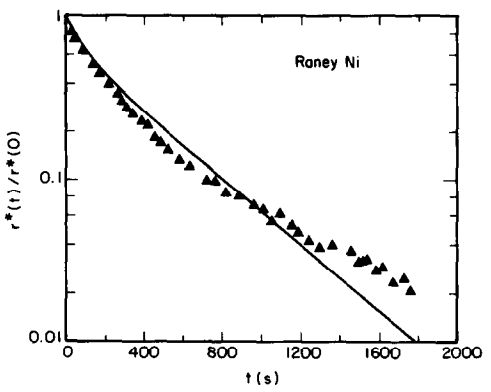

FIG. 8. An illustration of the fit of Eq. (12) to the data of Soong *et al.* (*14*).

illustrates the results of an unweighted least-squares fit to the data obtained using Eq. (12) (*14*)

$$r^*(t)/r^*(0) = A \exp(-k_{C_\alpha} t) + (1 - A) \exp(-k_{C_\beta} t). \quad (12)$$

It is evident that this equation cannot represent the data accurately over the full time domain. The values of k_{C_α} and k_{C_β} obtained by a nonlinear regression on all three parameters in Eq. (13) are given in Table I. The differences between the values of k_1 and k_2 we have obtained and those reported by Soong *et al.* (*14*) are very likely due to the different methods of curve fitting.

The plots of $f(k)$ presented in Figs. 4, 5, and 7 each exhibit two peaks. An interesting question to ask is whether the width of these peaks reflects the heterogeneity of the reactivity in C_α and C_β, or, instead the resolution limits in k imposed by the noise in the experimental data. To address this question, we recall that the resolution in k is controlled by ω_{max} (see Eq. (6)) which in turn is determined by ε (see Eq. (8)). For heterogeneity in sites to be observable the width of the peaks in $f(k)$ should be broader than that predicted by the resolution limit. This criterion can be expressed as

$$\log (k_+/k_-) > \pi/\omega_{max}, \quad (13)$$

where k_+ and k_- are the values of k for which the peak in $f(k)$ has half its maximum value. The values of $\log(k_+/k_-)$ estimated from the data in Figs. 4, 5, and 7 are comparable to π/ω_{max}. Consequently, it is not possible to draw any conclusions about the extent to which site heterogeneity contributes to the breadth of the peaks seen in these figures. To do so requires that the noise in the data be reduced below $\sim 10^{-3}$.

In closing, it is important to stress that the method of data analysis presented here is based on the assumption that each form of carbon on the catalyst undergoes hydrogenation to methane independently of all other forms. This assumption must be valid if the peaks in $f(k)$ are to be ascribed to specific forms of carbon, as has been done here. If the assumption is not valid, then the peaks in $f(k)$ will be indicative of a reaction scheme exhibiting identifiable grouping of rate coefficients, but it will not be possible to associate the peaks with particular forms of carbon.

CONCLUSIONS

In this paper we have shown how transient response curves obtained from isotopic tracer experiments can be analyzed to extract the maximum amount of information concerning the reactivity of carbon deposited during CO hydrogenation over Group VIII metals. The method assumes that different carbon forms can react independently to form methane and that the reactivity of each form is characterized by a first-order rate coefficient, k. The distribution of rate coefficients, $f(k)$, is obtained from an analysis of experimental transient response curves. Application of the method to data for Ru and Ni catalysts reveals the presence of two well defined peaks in $f(k)$, which can be associated with C_α and C_β forms of surface carbon. The resolution in defining these peaks is set by the noise in the data. For the noise present in the data analyzed, it is not possible to determine the extent to which the breadth in the peaks in $f(k)$ is due to a heterogeneity in carbon environments.

APPENDIX

McWhirter and Pike (*20*) have shown that there exists an orthogonal set of eigenfunctions, $\psi_\omega(k)$, and eigenvalues, λ_ω, such that

$$\int_0^\infty \psi_\omega(k)e^{-kt}dk = \lambda_\omega\psi_\omega(t). \quad \text{(A1)}$$

The eigenfunctions can be expressed in terms of the gamma functions $\Gamma(\frac{1}{2} \pm i\omega)$ and the eigenvalues have the form

$$\lambda_\omega = \frac{\omega}{|\omega|}\sqrt{\frac{\pi}{\cosh(\pi\omega)}}. \quad \text{(A2)}$$

Expansion of the function $kf(k)$ in terms of the continuous complete set of eigenfunctions gives

$$kf(k) = \int_{-\infty}^{\infty} a_\omega\psi_\omega(k)d\omega. \quad \text{(A3)}$$

Equation (A3) can now be used to rewrite Eq. (3) as

$$r^*(t) = \theta_0^* \int_{-\infty}^{\infty} a_\omega\lambda_\omega\psi_\omega(k)d\omega. \quad \text{(A4)}$$

From Eq. (A2) we see that as $\omega \to \infty$, $\lambda_\omega \to 0$, which means that for large values of ω (say $\omega > \omega_{max}$) the eigenfunctions are transmitted so weakly across Eq. (A4) that they cannot be distinguished from the noise of the experimental points, $\varepsilon(t)$. We can then rewrite Eq. (A4) as

$$r^*(t) = \theta_0^* \left[\int_{-\omega_{max}}^{\omega_{max}} a_\omega\lambda_\omega\psi_\omega(t)d\omega + \int_{\omega>\omega_{max}} a_\omega\lambda_\omega\psi_\omega(t)d\omega\right] + \varepsilon(t). \quad \text{(A5)}$$

where the second term on the right side is of the same order of magnitude as the noise $\varepsilon(t)$ and cannot be used to recover the function $kf(k)$. Accordingly, Eq. (A3) can be approximated by

$$kf(k) \simeq \int_{-\omega_{max}}^{\omega_{max}} a_\omega\psi_\omega(k)d\omega, \quad \text{(A6)}$$

with ω_{max} being defined by

$$\lambda_{\omega_{max}} \sim \varepsilon. \quad \text{(A7)}$$

By using the explicit functional form of $\psi_\omega(k)$ (*20*) and the definition

$$F(\log k)d(\log k) = kf(k)dk, \quad \text{(A8)}$$

Eq. (A6) can be rewritten as

$$\exp(-\tfrac{1}{2}\log k)F(\log k) = \int_{-\omega_{max}}^{\omega_{max}} \beta(\omega)\exp(i\,\omega\log k)d\omega, \quad \text{(A9)}$$

where $\beta(\omega)$ is a linear combination of a_ω and $a_{-\omega}$. The function on the left side of Eq. (A9) is a band-limited Fourier transform for which the sampling theorem (*24*) applies. The function $\exp(-\frac{1}{2}\log k)F(\log k)$ can, therefore, be fully reconstructed from the knowledge of its values at points $\log k_n$, $\log k_{n+1}$, etc. separated by π/ω_{max} using the interpolation formula

$$\exp(-\tfrac{1}{2}\log k)F(\log k) = \sum_{n=1}^{\infty} \exp(-\tfrac{1}{2}\log k_n)F(\log k_n) \times \frac{\sin[\omega_{max}\log(k/k_n)]}{\omega_{max}\log(k/k_n)}, \quad \text{(A10)}$$

with

$$k_n = \exp\left(\frac{\pi}{\omega_{max}}\right)k_{n-1}. \quad \text{(A11)}$$

In practice, a finite upper limit $n = N$ is used. Attempting to increase the resolution in $F(\log k)$ by spacing the values of $\log k_n$ more closely than π/ω_{max} is equivalent to extracting information from data below the noise level, and leads to unreliable results (*22*).

Assuming that $F(\log k)$ is defined on the interval $[\log k_1, \log k_N]$, then $r^*(t)$ can be written as

$$r^*(t) = \theta_0^* \int_{\log k_1}^{\log k_N} \exp(-kt)F(\log k)d(\log k). \quad \text{(A12)}$$

Introducing Eq. (A10) into Eq. (A12) gives

$$r^*(t) = \theta_0^* \sum_{n=1}^{\infty} \frac{\pi}{\omega_{max}} F(\log k_n) \exp(-k_n t)W_{\omega_{max}}(k_n, t), \quad \text{(A13)}$$

where

$$W_{\omega_{max}} = \int_{\log k_1}^{\log k_N} \exp[-t(k - k_n)] \frac{\exp[\frac{1}{2}\log(k/k_n)]\sin[\omega_{max}\log(k/k_N)]}{\pi \log(k/k_n)}. \quad (A14)$$

Equations (A13) and (A14) are equivalent to Eqs. (5) and (7) in the text.

ACKNOWLEDGMENTS

The authors are indebted to Professor Erdogan Gulari for drawing their attention to the analytical method described in this paper and for subsequent discussions of its application to problems in transient response kinetics. The work reported here was supported by the Office of Basic Energy Sciences, Chemical Sciences Division of the U.S. Department of Energy, under Contract DE-AC03-76SF00098 and Exxon Research and Engineering Company. Support for M. de Pontes was received from the Assistant Secretary of Fossil Energy, Office of Coal Research, University Contracts Division of the U.S. Department of Energy, under Contract W-7405-ENG-48.

REFERENCES

1. Ponec, V., and van Barneveld, W. A., *Ind. Eng. Chem. Prod. Res. Dev.* **18,** 268 (1979).
2. Bell, A. T., *Catal. Rev. Sci. Eng.* **23,** 203 (1981).
3. Biloen, P., and Sachtler, W. M. H., *Adv. Catal.* **30,** 165 (1981).
4. Wentrcek, P. R., Wood, B. J., and Wise, H., *J. Catal.* **43,** 363 (1976).
5. Araki, M., and Ponec, V., *J. Catal.* **44,** 439 (1976).
6. Biloen, P., Helle, J. N., and Sachtler, W. M. H., *J. Catal.* **58,** 95 (1979).
7. Cant, N. W., and Bell, A. T., *J. Catal.* **73,** 257 (1982).
8. Kobori, Y., Yamasaki, H., Naito, S., Onishi, T., and Tamaru, K., *J. Chem. Soc. Faraday Trans. 1* **78,** 1473 (1982).
9. Happel, J., Cheh, H. Y., Otarod, M., Ozawa, S., Severdia, A. J., Yoshida, T., and Fthenakis, V., *J. Catal.* **75,** 314 (1982).
10. Biloen, P., Helle, J. N., van den Berg, F. G. A., and Sachtler, W. M. H., *J. Catal.* **81,** 450 (1983).
11. Winslow, P., and Bell, A. T., *J. Catal.* **86,** 158 (1984).
12. Winslow, P., and Bell, A. T., *J. Catal.* **91,** 142 (1985).
13. Winslow, P., and Bell, A. T., *J. Catal.* **94,** 385 (1985).
14. Soong, Y., Krishna, K., and Biloen, P., *J. Catal.* **97,** 330 (1986).
15. Duncan, T. M., Winslow, P., and Bell, A. T., *J. Catal.* **93,** 1 (1985).
16. Duncan, T. M., Reimer, J. A., Winslow, P., and Bell, A. T., *J. Catal.* **95,** 305 (1985).
17. Goodman, D. W., and Yates, Jr., J. T., *J. Catal.* **82,** 255 (1983).
18. Scott, K. F., *J. Chem. Soc. Faraday Trans. 1* **76,** 2065 (1980).
19. Herschel, R., "A Guide to the Application of the Laplace and Z Transforms," Van Nordstrand-Rheinhold, New York, 1971.
20. McWhirter, J. G., and Pike, E. R., *J. Phys. A* **11,** 1729 (1978).
21. McWhirter, J. G., *Opt. Acta* **27,** 83 (1980).
22. Ostrowsky, N., Sornette, D., Parker, P., and Pike, E. R., *Opt. Acta* **28,** 1059 (1981).
23. Yokomizo, G. H., and Bell, A. T., unpublished results.
24. Woodward, P. M., "Probability and Information Theory with Application to Radar," Pergamon, Oxford, 1964.